Enhanced Hall slope in wide $Al_xGa_{x-1}As$ parabolic wells

A. M. Ortiz de Zevallos, N. C. Mamani, G. M. Gusev, A. A. Quivy, and T. E. Lamas
Instituto de Física da Universidade de São Paulo, CP 66318, CEP 05315-970 São Paulo, São Paulo, Brazil

J. C. Portal
GHMFL-CNRS, BP-166, F-38042 Grenoble, Cedex 9, France; INSA-Toulouse, Toulouse 31077, Cedex 4, France; and Institut Universitaire de France, Toulouse, France

(Received 26 December 2006; revised manuscript received 23 March 2007; published 15 May 2007)

We report measurements of the Hall effect in 1000–4000 Å wide $Al_xGa_{x-1}As$ parabolic wells with quasi-two-dimensional electrons and holes in a perpendicular magnetic field. Above a critical magnetic field $B > 3T$, the Hall resistance for wide parabolic wells is found to be enhanced when the temperature decreases. We attribute this enhanced Hall slope to a carrier density effect. The Hartree and exchange-correlation terms produce a strong variation of the potential-well shape. The width of the electronic and hole slabs shrinks as the magnetic field is increased, which leads to the redistribution of the charge between the well and impurity layer.

DOI: 10.1103/PhysRevB.75.205324 PACS number(s): 73.21.Fg, 72.20.My, 71.45.−d

I. INTRODUCTION

Remotely doped parabolic quantum wells (PQWs) were initially proposed as a system where it might be possible to observe broken-symmetry ground states for a three-dimensional (3D) electron system in the presence of a strong magnetic field.[1] In such PQW, the electrons are spatially separated from the dopant atoms, and this reduces electron impurity scattering and provides an opportunity to study a clean interacting electron system. In addition, parabolic wells are considered more attractive for theoreticians, because the electrons screen the bare parabolic potential and form a constant density slab, which is a good approximation to a three-dimensional jellium, where electrons move in a constant background positive charge density.

The discovery of the fractional quantum Hall effect demonstrated the importance of the Coulomb interactions for two-dimensional (2D) electron systems in the last Landau level.[2] Another famous example is the formation of stripe charge-density wave (CDW) phases in high Landau levels[3] at half-integer filling factor $\nu=N+1/2$. Within the Hartree-Fock framework, Brey[4] proposed a possible exchange induced charge-density wave state in a wide PQW subjected to a perpendicular magnetic field at Landau filling factor $\nu=1$. Recently, the magnetoplasmon excitations have been calculated in parabolic wells in a tilted magnetic field.[5] Several exotic symmetry-broken states, such as skyrmion stripe phases, have been predicted.[6] In contrast to narrow quantum wells and heterojunctions, in wide PQW, such a phase transition has not been observed experimentally. The absence of the CDW instability in n-type $Al_xGa_{1-x}As$ parabolic wells can be attributed to the relatively low level of the electron-electron interaction strength, a small moderate dimensionless parameter r_s value, and low mobility. The 2D holes are characterized by a larger r_s, usually >10, due to the heavy effective mass; however, the hole mobility is lower than for electrons.

It is worth noting that some of the many-body effects in a wide electronic slab may be robust against electron impurity scattering. Previous numerical computations of the charge distribution and potential-well shapes as a function of magnetic field demonstrated that the Hartree and exchange-correlation terms are equally important as the bare potentials in the Schrödinger equation.[7] In particular, as the magnetic field is increased, the width of the electron slab shrinks and the minima of the self-consistent potential near the edges of the electron slab are shifted to the center of the well. This may lead to a decrease of the electron density n_s in the well, since n_s is very sensitive to the well potential shape.

In this paper, we report measurements of the Hall resistance in wide electronic and hole parabolic wells in a perpendicular magnetic field. We found that above a critical magnetic field, the Hall slope for hole systems is strongly enhanced in comparison with the low-field Hall coefficient. Electronic parabolic wells with the same slab width demonstrate normal behavior; however, the Hall slope is enhanced for wider wells. We attribute this effect to a decrease in charge density due to the shrinking of the slab width inside the bare parabolic potential.

II. EXPERIMENTAL RESULTS

Taking z as the growth direction and taking $z=0$ the center of parabolic well, we consider an effective harmonic potential $V_0(z)=m\Omega^2z^2/2$, with $\Omega=c(2/m)^{1/2}$ and effective mass m, for a composition profile $x(z)=cz^2$. The characteristic bulk density is given by $n_+=\frac{\Omega^2m^*\varepsilon}{4\pi e^2}$. The effective thickness of the electronic slab can be obtained from $W_e=n_s/n_+$, where n_s is the two-dimensional density. For a partially filled quantum well, W_e is smaller than the geometrical width of the well W, and we define a filling factor at zero magnetic field as $f=W_e/W$. Figure 1 illustrates the conduction-band profile for an empty and a partially full parabolic well. When several subbands become occupied, the potential profile broadens and turns into the square-well profile with corresponding square-well energy levels $E_0=(2\pi)^2\hbar^2/(8mW_e^2)$. Note that when one subband is occupied, the Fermi energy E_F increases linearly with n_s, as for 2D system. However, for parabolic wells with two or three occupied subbands, the Fermi energy is nearly constant and does not vary with surface density. This follows from the fact that the width of the electron slab W_e increases with n_s, so that the bulk density

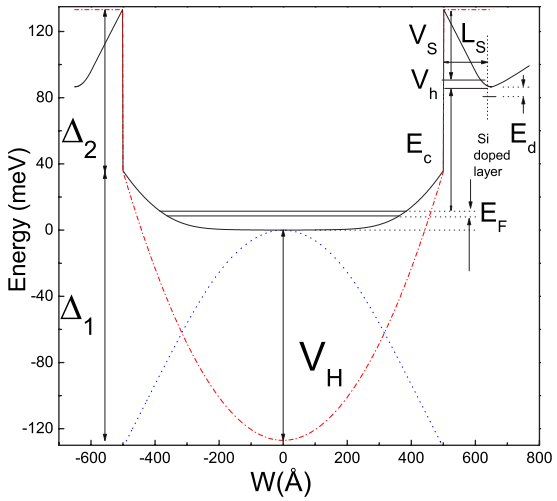

FIG. 1. (Color online) Illustration of the conduction-band edge in an empty parabolic well and partially full PQW with $W=1000$ Å and $L_s=100$ Å. Δ_1 is the height of the parabolic well, Δ_2 is the height of the $Al_xGa_{x-1}As$ barrier, L_s is the spacer width, E_F is the Fermi energy, V_H is the band bending energy resulting from electron-electron interactions, E_c is the highest occupied energy level, E_d is the activation energy of donor impurities, V_s is the depletion energy of the ionized charge, and V_h is the potential of the donor layer. The dashed line (---) shows the potential without charge, the dash-dotted line (-·-) is the potential due to electron-electron interactions, and the total self-consistent potential is represent by a solid line (—).

$n_+=n_s/W_e$ remains essentially constant.[8,9] For a full parabolic well, we have

$$E_F=\hbar^2(3\pi^2N_+)^{2/3}/(2mW^{4/3}), \tag{1}$$

where $N_+=n_+W^2$. It is worth noting that the 3D approximation is also valid for filling fractions $f\sim 0.2-0.3$. We therefore use Eq. (1) for the estimation of the interaction parameter r_s in our samples. The dimensionless interelectron spacing in the 3D case is given by $r_s=\frac{4\pi^2m^*e^2}{\varepsilon\hbar^2}\left(\frac{3}{4\pi n_+}\right)^{1/3}$. The parameter r_s is much larger in p-type parabolic quantum well due to their large effective mass; therefore, many-body effects are expected to be more pronounced in three-dimensional hole systems. From Table I, we may see that the dimensionless parameter $r_s\approx 15$ for 3000 Å wide PQW with holes ($m^*=0.4m_0$) and 3.3 for electronic 4000 Å wide well. Realistic wells are characterized by the three parameters shown in Fig. 1: the height Δ_1 and the width W of the parabolic well and the height of the $Al_xGa_{x-1}As$ barrier Δ_2. The harmonic potential frequency is connected with the height of the parabola by the simple equation $\Omega=(8\Delta_1/mW^2)^{1/2}$.

The p-type samples were grown by a molecular-beam epitaxy technique on semi-insulating (311)A substrates. Several samples were grown with a PQW width $W=1000-3000$ Å and symmetrically doped with silicon located at 150 or 200 Å from their border. We observed a systematical decrease of the hole density in the PQW with an increase of the width: the density went from 3.7×10^{11} cm^{-2} for $W=1000$ Å sample to 1.7×10^{11} cm^{-2} for $W=3000$ Å quantum well. The n-type samples were grown on semi-insulating (100) substrates. A summary of the samples parameters is shown in Table I. The effective thickness of the hole slab was $W_h=p_s/p_+\approx 800$ Å for 2000 Å PQW and $W_h\approx 500$ Å for the $W=1000$ Å sample. Some of the details of the crystal growth are reported in Ref. 10. The mobility of the holes was of the order $(30-60)\times10^3$ cm^2/V s at $T=1.4$ K and increased up to 100×10^3 cm^2/V s at $T=50$ mK. The measurements in this study were performed using Hall bar geometry with current flow in the $[\bar{2}33]$ and the $[01\bar{1}]$ directions for p-type structures. The samples were immersed in the mixing chamber of a top-loading dilution refrigerator with a base temperature $T=50$ mK. We measured magnetoresistance and Hall resistance in perpendicular magnetic fields employing a

TABLE I. The sample parameters.

Sample	Orientation	Carrier type	Spacer (Å)	W (Å)	n^+ (10^{16} cm^{-3})	n_s (10^{11} cm^{-2})	n_s^* (10^{11} cm^{-2})	r_s	W_{eff} (Å)	μ (cm^2/V s)
2384	100	Electrons	200	1000	8.8	4.6	4.33	1.53	520	170000
2384	(311)A	Holes	200	1000	8.8	3.7		8.4	420	62000
2577	100	Electrons	200	1000	11.9	4.2	4.33	1.4	353	353000
2378	100	Electrons	500	1000	11.9	2.3	2.8	1.4	190	153000
2496	100	Electrons	200	1500	5.3	3.5	3.52	1.8	650	140000
2496	(311)A	Holes	200	1500	5.3	2.44		10	460	53000
2496	(311)A	Holes	200	1500	5.3	2.4		10	450	53000
2535	100	Electrons	200	1700	4.1	3.2	2.96	2	784	220000
2385	(311)A	Holes	150	2000	3	2.4		12	800	43000
2499	(311)A	Holes	150	2000	3	2.4		12	800	37000
2500	(311)A	Holes	150	2500	3	2.2		12	730	32000
2518	(311)A	Holes	150	2500	3	2.4		12	800	35000
2386	100	Electrons	150	3000	2.2	2.9	3.07	2.4	910	118000
2386	(311)A	Holes	150	3000	1.3	1.7		15.9	1310	57000
$AG662$	100	Electrons	100	4000	0.88	1.5	1.71	3.3	1700	120000

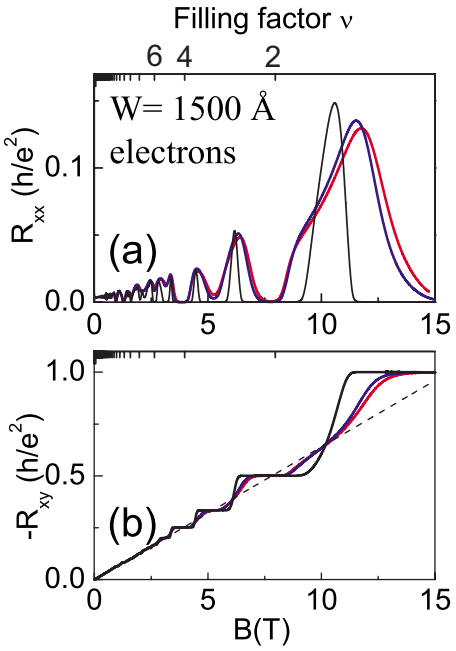

FIG. 2. (Color online) (a) Magnetoresistance and (b) Hall resistance of a 1500 Å PQW with electrons as a function of the perpendicular magnetic field for different temperatures T (mK): 850 (red), 650 (blue), 50 (black). The dashed line (---) corresponds to a linear extrapolation of low-field Hall resistance.

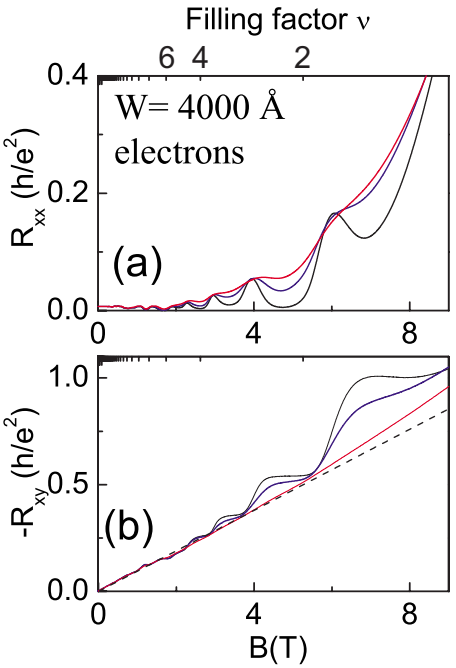

FIG. 3. (Color online) (a) Magnetoresistance and (b) Hall resistance of a 4000 Å PQW with electrons as a function of the perpendicular magnetic field for different temperatures T (mK): 950 (red), 450 (blue), 50 (black). The dashed line (---) corresponds to a linear extrapolation of low-field Hall resistance. Sample was illuminated by red-light-emitting diode.

standard low-frequency (6–13 Hz) lock-in technique. We found I-V nonlinearity for wide p-type parabolic well in the quantum Hall-effect regime for current $I > 10^{-9}$ A. We suspect that this effect is not due to the heating but rather indicates the beginning of the CDW instability (see discussions). Therefore, we applied the current between 10^{-7} and 10^{-9} A in order to minimize the heating and nonlinear effects.

In Fig. 2, we show plots of longitudinal R_{xx} resistance of 1500 Å wide electronic parabolic well versus perpendicular magnetic field for three different temperatures. We can see that the electrons demonstrate conventional quantum Hall-effect (QHE) behavior: wide plateaus in the Hall resistance accompanied by deep minima in R_{xx}. Note that the Hall resistance is linear with magnetic field and that the center of the Hall plateaus coincides with the center of the minima in R_{xx}. Several electronic samples with the parameters indicated in Table I from different wafers with different widths were studied, and all have demonstrated conventional QHE and linear Hall resistance. Figure 3 shows typical traces of R_{xx} and R_{xy} for a 4000 Å wide electronic parabolic well as a function of magnetic field for different temperatures. This sample was illuminated in order to achieve a wider width of the electronic slab and a filling fraction $f \approx 1$. We observe that the Hall resistance varies linearly with magnetic field at low B, but that at higher field, R_{xy} deviates from linearity, and that its slope increases. Note that the extrapolation of the low B Hall resistance intersects the Hall plateaus at magnetic field higher than the centers of the plateaus. Such anomalous behavior is observed only at low temperature, at $T > 2$ K, the linearity of R_{xy} is recovered and compatible with the ordinary Hall effect.

Parabolic wells with holes, in general, demonstrated similar behavior. However, an enhanced Hall slope is observed in samples with smaller effective width. Figure 4 illustrates the dependence of the Hall resistance on the sample width W for p-type PQW. We see that the Hall resistance for $W = 1500$ Å wide parabolic well clearly deviates at $B \approx 4$ T from the former low field linear dependence. Figures 5 and 6 show the very pronounced high-field excess Hall resistance in 2000 and 2500 Å parabolic wells. Note that the Hall slope is changed abruptly at a critical magnetic field $B_c \approx 3.2$ T and cannot be accounted for by a simple gradual magnetic freeze-out picture. Generally, such behavior may be described by

$$R_{xy} = A(B - B_0)/ep_s, \tag{2}$$

where B_0 and A are temperature-dependent coefficients. The Hall slope $R_H = \Delta R_{xy}/\Delta B$ gradually increases when temperature decreases and becomes two times larger at $T = 50$ mK than at low field and high temperatures. Figure 7 shows the longitudinal and Hall resistances close to the critical magnetic field. We see that above the critical field, the Hall resistance increases when the temperature decreases, which corresponds to the metal-insulator transition behavior.

Now, we analyze the correlation between the Hall resistance and longitudinal transport. In the quantum Hall-effect regime, the minima in R_{xx} coincide with the center of the Hall plateaus, which have the value $h/\nu e^2$, where ν is the Landau filling factor. From Figs. 3–6, we see that the excess Hall resistance is observed to occur for small Landau filling factors $\nu < 3$, which makes it difficult to identify the corresponding minima in R_{xx}. Note that for holes, the quantum

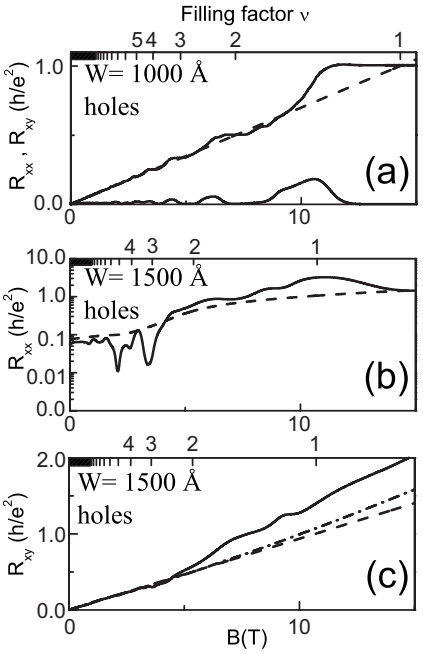

FIG. 4. (a) Magnetoresistance and Hall resistance of a 1000 Å PQW with holes as a function of the perpendicular magnetic field, $T=50$ mK. The dashed line corresponds to a linear extrapolation of the low-field Hall resistance. (b) Magnetoresistance and (c) Hall resistance of a 1500 Å PQW with holes versus B for two temperatures T (mK): 950 (---, dash-dotted line) and 50 (—, solid line). The dashed line (---) corresponds to a linear extrapolation of low-field Hall resistance.

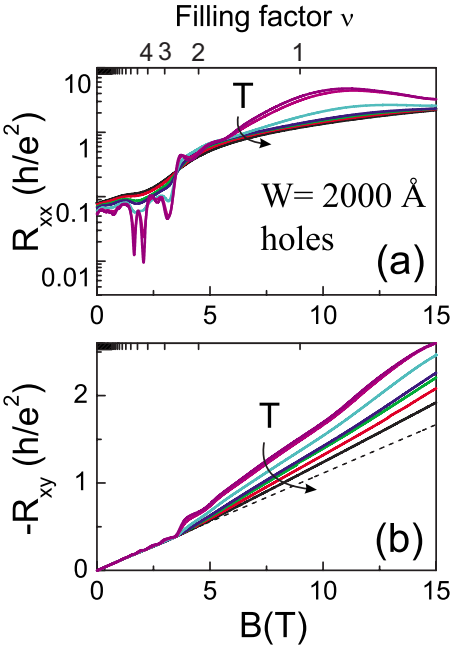

FIG. 5. (Color online) (a) Magnetoresistance and (b) Hall resistance of a 2000 Å PQW with holes versus B for different temperatures T (mK): 1000 (black), 950 (red), 700 (green), 360 (blue), 200 (cyan), 150 (magenta), and 50 (purple). The dashed line (---) corresponds to a linear extrapolation of the low-field Hall resistance. R_{xx} in logarithmic scale.

Hall features are not observed: R_{xx} shows a maximum instead of a minimum, and the plateau in R_{xy} is absent. We suggest that the $\nu=1$ minimum is suppressed because the spin gap (or intersubband energy separation) is too small. The g factor in p-type GaAs system is unknown and, in principle, can be small, in which case the gap will be hardly resolved due to the low mobility. A second scenario which may be suggested is the formation near $\nu=1$ of the isotropic-spin- or charge-density state proposed by Brey[4] for a sufficiently thick electron slab, $W_h > W_c$. Brey considered the static linear response of the thick electron layer in the presence of the interactions and high magnetic fields and found that it has a soft mode which can be interpreted as a beginning of a CDW instability. Below, we will focus mostly on the Hall-effect behavior, and we believe that the interpretation of the longitudinal resistance is not necessary for the explanation of the excess Hall resistance.

In Fig. 6, we see the deep minima in R_{xx} at $B=12$ T and the corresponding plateau in the enhanced $R_{xy}=3h/e^2$, which can be attributed to the fractional Hall effect at $\nu=1/3$. However, from an extrapolation of the low-field Hall resistance, a $1/3$ fraction is expected for a much higher field $B\approx 25$ T. It is worth noting that the observation of the fractional Hall effect in low mobility sample ($\mu\approx 70\times 10^3$ cm^2/V s at $T=50$ mK) is not very surprising, and similar observations have been reported in p-type $Al_xGa_{1-x}As$ heterostructures[11] and AlAs quantum well[12] for electrons with a large effective mass.

We attribute the enhanced R_H to a varying carrier density effect. Since the shape of the wave function in the z direction and potential profile are very sensitive to the electron-electron interaction and may be tuned by strong magnetic fields, the result is the redistribution of the charge between the well and dopant layers. The evolution of the shape of the electron-gas slab and the self-consistent potential of a parabolic quantum well with magnetic field have been studied in Refs. 7 and 13. Below, we reproduce these results and cal-

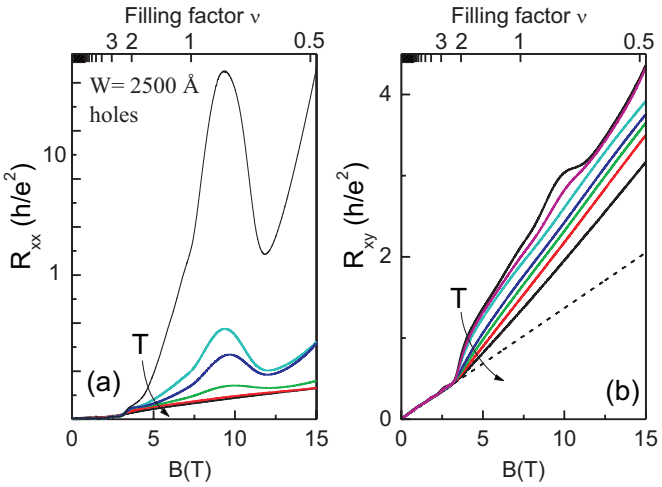

FIG. 6. (Color online) (a) Magnetoresistance and (b) Hall resistance of a 2500 Å PQW with holes versus B for different temperatures T (mK): 1000 (black), 950 (red), 700 (green), 360 (blue), 200 (cyan), 150 (magenta), and 50 (purple). The dashed line (---) corresponds to a linear extrapolation of the low-field Hall resistance. R_{xx} in logarithmic scale.

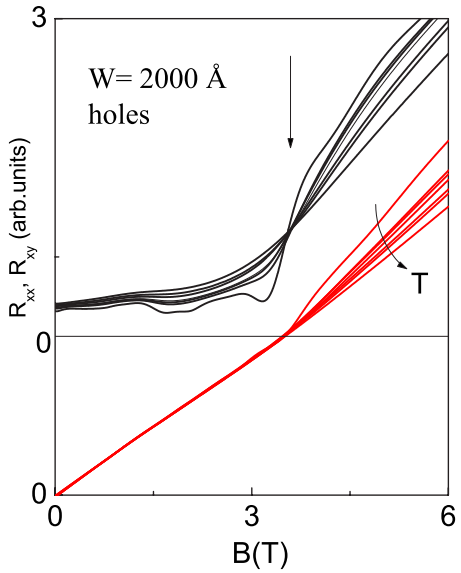

FIG. 7. (Color online) The longitudinal (black) and Hall (red) resistances as a function of magnetic field for different temperatures T (0.1, 0.2, 0.3, 0.4, 0.6, 0.8, and 1.0 K). Arrow shows the critical magnetic field, above which the Hall resistance becomes temperature dependent.

culate the sheet density in parabolic wells in zero and strong magnetic fields.

III. WIDE PARABOLIC WELL IN ZERO MAGNETIC FIELD: SELF-CONSISTENT AND ANALYTICAL CALCULATIONS

We begin with the calculation of the ground-state electron density and the self-consistent potential for an ideal electronic parabolic well in the Hartree approximation for well parameters which are close to the experimental samples. We studied PQW with widths between 1000 and 4000 Å with a depth $\Delta_1=661(1.55x+0.37x^2)$ meV for the parabolic potential and an additional spacer barrier $\Delta_2=661[1.55(y-x)+0.37(y-x)^2]$ meV. Carriers into the well are supplied by dopant layers located at both sides of the well. These are located after the spacer layer (L_s) of undoped $Al_xGa_{1-x}As$ (Fig. 1). Dopant layers have 2.5×10^{-12} cm^{-2} of surface density and a thickness of 50 Å. This width for the dopant layer was used because, as was shown by Schubert *et al.*,[14] for the growth conditions of our samples, the δ-doped Si layer diffuses to a width of 50 Å and we are considering modulation doping in our calculations.

Figure 1(b) shows the results of such a calculation for a PQW with $W=1000$ Å, sheet density of $n_s=5.45\times10^{11}$ cm^{-2}, and spacer layer of $L_s=100$ Å. In our approximation, we suppose that electrons from δ-Si layer are transferred into the well until the system achieves thermodynamical equilibrium. In this case, a charge balance equation[15] can be written:

$$V_p = V'_H + E_c + E_F + E_d + V_h + V_s, \tag{3}$$

where $V_p=\Delta_1+\Delta_2$ is the sum of the height of the parabolic potential Δ_1 and the spacer barrier Δ_2, V_H is the band bending energy resulting from electron-electron interactions, E_c is the highest occupied energy level, E_d is the activation energy of donor impurities, V_s is the depletion energy of the ionized charge, and V_h is the potential of the donor layer.

Analytical expression for the electron density can be obtained from first-order perturbation theory, if we assume that only the two lowest subbands are populated.

When two bands are occupied with total density $n_s=n_0+n_1$, where n_0 and n_1 are the densities of the first and the second subband, the Poisson equation is given by

$$\frac{d^2V'}{dz^2} = \frac{e^2}{\epsilon}n(z) = \frac{e^2}{\epsilon}[n_0\phi_0(z) + n_1\phi_1(z)], \tag{4}$$

where the potential $V'(z)$ can be determined from

$$V'(z) = -\frac{e^2n_s}{2\epsilon}\left[z\,\mathrm{erf}(\sqrt{a}z) + \frac{1}{\sqrt{a\pi}}(e^{-az^2}-1)\right] - \frac{e^2n_1}{2\epsilon}\left[\frac{1}{\sqrt{a\pi}}(e^{-az^2}-1)\right], \tag{5}$$

where the erf function is the Gauss error function and $a=m^*\Omega/\hbar$. The functions $\phi_0(z)$ and $\phi_1(z)$ are the harmonic oscillator wave functions for $n=0$ and $n=1$,

$$\phi_0(z) = \left[\frac{a}{\pi}\right]^{1/4} e^{-az^2/2},$$

$$\phi_1(z) = \left[\frac{a}{\pi}\right]^{1/4} \sqrt{2a}ze^{-az^2/2}. \tag{6}$$

The eigenenergies of the Hamiltonian $H+V(z)$ were calculated in the basis of two bound states. It can be written as

$$\begin{bmatrix} E_0+\delta E_0 & V_{01} \\ V_{01} & E_1+\delta E_1 \end{bmatrix}, \tag{7}$$

where

$$\delta E_n = \langle\phi_n|V|\phi_n\rangle,$$

$$V_{nj} = V_{jn} = \langle\phi_n|V|\phi_j\rangle. \tag{8}$$

The nondiagonal elements $V_{nj}=V_{jn}$ are zero since ϕ_n and ϕ_j have different parities. We calculated the confinement energies in the first and second subbands, and finally from the charge balance equation [Eq. (3)], we determined the density of the electrons in the parabolic well, assuming $n_1 \ll n_0$:

$$n_s = \frac{V_p - \hbar\Omega - E_d}{\frac{e^2}{\epsilon}\left[\frac{W\,\mathrm{erf}\left(\frac{\sqrt{a}W}{2}\right)}{4} - \frac{1}{2\sqrt{a\pi}} + \frac{5\,\mathrm{erf}\left(\frac{\sqrt{2a}W}{2}\right)}{2\sqrt{2a\pi}} - \frac{\mathrm{erf}\left(\sqrt{\frac{2aW}{2}}\right)}{\sqrt{a\pi}} + \frac{W}{\pi}e^{-aW^2/4}(e^{-aW^2/4}-1) + \frac{L_s\epsilon}{2\epsilon_1}\right] + \frac{\pi\hbar^2}{2m^*}}. \quad (9)$$

As we mentioned above, we performed self-consistent calculations of the energy spectrum of the electronic states in the parabolic well. We do not consider the effective-mass variation across the well resulting from the variation of the Al concentration. Including these effects into a more complete theory[16] may improve quantitative agreement with experiments. The wave functions Φ_i^n and energies E_i^n can be found from the Schrödinger equation

$$-\frac{\hbar^2}{2m^*}\frac{d^2}{dz^2}\Phi_i^n(z) + [V_0(z) + V_H(z) + V_{XC}(z)]\Phi_i^n(z) = E_i^n\Phi_i^n(z). \quad (10)$$

In this equation, V_H is the Hartree potential given by

$$V_H = -\frac{2\pi e^2}{\varepsilon_{sc}}\int_{-\infty}^{\infty} dz' n(z')|z - z'|, \quad (11)$$

and exchange-correlation potential

$$V_{XC} = -0.985\frac{e^2}{\varepsilon_{sc}}n(z)^{1/3} \times\left\{1 + \frac{0.022\,85}{a_B^* n(z)^{1/3}}\ln[1 + 33.852a_B^* n(z)^{1/3}]\right\}. \quad (12)$$

In these expressions, $n(z)$ is the electron density, ε_{sc} is the dielectric constant, and $a_B^* = \varepsilon_{sc}\hbar^2/m^* e^2$ is the effective Bohr radius.

We also used a self-consistent calculation to find the charge transferred into the parabolic quantum wells. In this approximations, we again suppose that electrons from δ-Si layer are transferred into the well until the system achieves thermodynamical equilibrium (a uniform Fermi level), and as for the analytical approximation, we use the balance equation [Eq. (3)]. In Fig. 8, we compare the results of the self-consistent calculations, the analytical approximation, and the experimental results for different electronic parabolic wells. As expected, the self-consistent calculations show good agreement with experimental results.

We do not attempt to calculate the energy spectrum and the density variation in p-type wide parabolic quantum well because of the complexity of such calculations.[17,18] In the present work, we use a simple model to explain the Hall coefficient behavior in p-type parabolic wells. Figure 9 shows the experimental data and analytical approximations for two subbands. Indeed, as expected, the analytical formula underestimates the value of n_s, as for electronic PQW. However, it explains qualitatively the decrease of the hole density with the well width. Note that we modified Eq. (9) for p-type PQW, because the lowest subband is occupied by the heavy holes and the second is occupied by the light holes.[17,18]

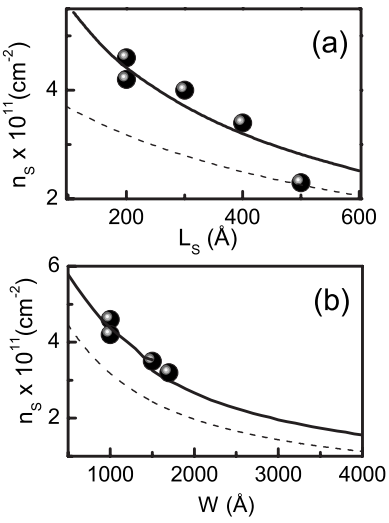

FIG. 8. (a) Variation of electronic density n_s in PQWs of width 1000 Å with spacer L_s. The solid circles are the experimental data, solid line (—) represent the self-consistent calculations, dashed line (…) is the analytical approximation for two subbands. (b) Variation of electronic density n_s in a PQWs with width for L_s=200 Å. The solid circles are the experimental data, solid line (—) represents the self-consistent calculations, and dashed line (…) is the analytical approximation for two subbands.

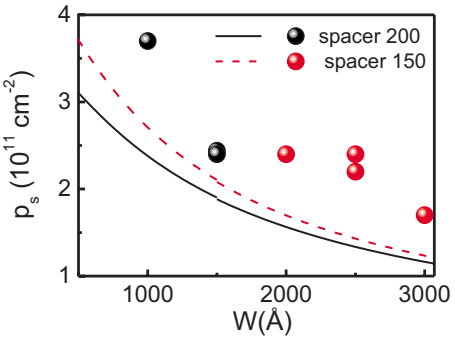

FIG. 9. (Color online) Variation of hole density p_s in PQWs with width for different spacer layers. The solid circles are the experimental data, and solid line and dashes represent the simple analytical approximation for two subbands.

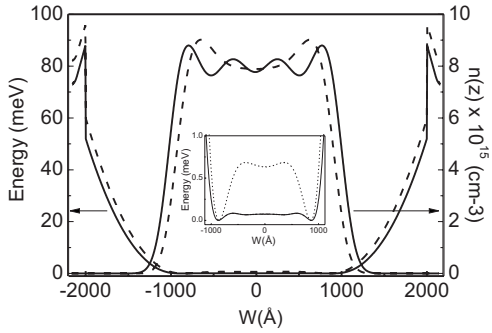

FIG. 10. Calculated total potential profile and electron density for a $W=4000$ Å PQW in the absence of magnetic field (solid line) and at $B=10$ T (dashes). Inset shows the bottom of the potential profile.

To conclude this part, we may emphasize here that the charge balance equation and the knowledge of the energy spectrum allow us to calculate the density of the charge carriers in the wide PQW with different widths and spacers in zero magnetic field. We now calculate the density in strong magnetic fields.

IV. WIDE PARABOLIC WELL IN MAGNETIC FIELD: SELF-CONSISTENT CALCULATION

We choose the magnetic field in the z direction and use the gauge $\mathbf{A}=(0,Bx,0)$. We assume that the XY-plane part of the wave function and the energy are the same as in the case of independent electrons:

$$\Psi_{n,i,k_y}(r)=\frac{1}{\sqrt{L}}e^{ik_y y}\varphi_n(x-k_y l_B^2)\Phi_i^n(z), \tag{13}$$

$$\epsilon_{n,i}=\left(n+\frac{1}{2}\right)\hbar\omega_c+E_i^n. \tag{14}$$

In Eq. (13), L is the sample dimension, φ_n are the eigenstates of the one-dimensional harmonic oscillator, $\omega_c=eB/m^*c$ is the cyclotron frequency, and $l_B=\sqrt{\hbar c/eB}$ is the magnetic length. The wave functions Φ_i^n and energies E_i^n can be found from the Schrödinger equation in the magnetic field. The electron-density profile in the well is given by

$$n(z)=\frac{1}{2\pi l_B^2}\sum_{n,i}\nu|\Phi_i^n(z)|^2, \tag{15}$$

where ν is the Landau filling factor of the state.

Figure 10 shows the electron-density profile and self-consistent potential for 4000 Å wide electronic parabolic well for zero magnetic field and at $B=10$ T. Note that the potential is not flat: it has two minima near the edges of the electronic slab and a maximum at the center of the well. We see that the magnetic field strongly modifies potential profile and density distribution, that the width of the electronic slab shrinks with field, and that the height of the central maximum of the self-consistent potential increases with field. These results reproduce previously reported shrinking of the electronic slabs in the wide parabolic wells in strong magnetic fields.[7,13] Hembree *et al.* attribute such modification of the electronic potential to the Hartree term in strong magnetic fields, which becomes equally important as the bare parabolic potential. We can also interpret such behavior as a precursor of the formation of the intersubband induced isotropic CDW state proposed by Brey[4] for a sufficiently thick electron slab $W_h > W_c$. For example, in electronic PQW with 4000 Å geometrical width W and characteristic energy $\hbar\Omega=5.7$ meV, a transition should occur at critical thickness $W_c \geqslant 700$ Å, which corresponds to the critical electron sheet density $n_s^c=2.1\times10^{11}$ cm^{-2}. Moreover, we cannot exclude the formation of a CDW state in p-type PQW. However, this effect may be destroyed by impurity scattering. Therefore, we found it more reasonable to explain the enhanced Hall slope in both n- and p-type PQWs by shrinking of the charge slab in the strong perpendicular magnetic field, which does not depend on impurity scattering effects.

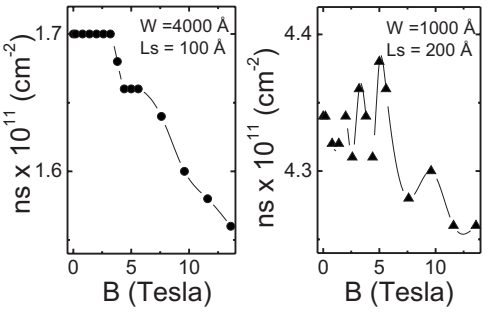

FIG. 11. Variation of the electron density with magnetic field for (a) a PQW with $W=4000$ Å and (b) a PQW with $W=1000$ Å.

The effective decrease of the width of the electron slab may lead to the increase of the distance between the electrons and impurity layer, which supplies the carriers into the well, and, consequently, leads to a decrease of the density in the well. We used self-consistent calculations of the energy spectrum and the balance equation in order to obtain the variation of the electronic density in wide PQW with magnetic field.

Figure 11 shows the density as a function of magnetic field for 4000 and 1000 Å wide electronic parabolic wells. We see a decrease of the density with B of up to 9% in the wide parabolic well and small ($\sim$1%) oscillations of the density in the narrow well. Note that in the 4000 Å wide well, the density is almost constant at $B<4T$, which agrees with our observation. This corresponds to magnetic field for which only the two last Landau levels are occupied.

It is extremely difficult to calculate the energy spectrum for p-type PQW in the strong magnetic field. In addition, the r_s factor for holes is very large, usually >10, as we can see in Table I. Note that the validity of the Hartree approximation may be limited to $r_s<1$ and that for larger r_s, the validity is no longer clear. Nevertheless, we believe that the usual Hartree approximation captures all essential physics and that for holes, the density variation effect can be even stronger than for electrons.

Our simple model does not explain the temperature effects, which are clearly seen in Figs. 5–7. Our calculations are performed at zero temperature, and it seems very likely that the finite temperature smears out interactions effects,

and a normal Hall slope is recovered at 1–2 K. We did not observe the intermediary stage of the ordinary Hall slope in the quantum regime. Temperature effects may smear out gradual change in the slope of the Hall effect with magnetic field.

Finally, we consider other phenomena which may explain the enhanced Hall factor in the two-dimensional systems. First, the presence of the carriers with different mobilities and densities may cause the changes in the Hall coefficient. However, this effect should lead to the ordinary Hall coefficient in strong magnetic fields and enhanced Hall coefficient at low B,[19] which is exactly the opposite of what we observed in experiments (see Fig. 5–7). Second, the temperature-induced Hall slope change has been predicted by the theory of the quantum corrections to the Hall resistivity which have recently been re-examined and reformulated in terms of elastic scattering of electrons by Friedel oscillations.[20] However, this theory cannot explain why the Hall slope starts to increase above a critical magnetic field, which is shown in Fig. 5–7. Note also that the value of the Hall resistance corrections, predicted by this theory,[20] is much smaller than we observed. Finally, we also tried to explain our observation by spin-dependent transport in wide parabolic wells. Recently, we reported the change in the Hall slope in a wide electronic PQW in a quasiparallel magnetic field.[21] We attributed the enhanced Hall slope in the presence of the parallel magnetic field to the suppression of the motion in the z direction in quasi-three-dimensional system. In AlGaAs PQW, the g factor is varied strongly along the z direction, and such motion requires a spin flip, which is suppressed by low temperature.

In spite of the similarity of the experimental curves, we should emphasize many differences between these two observations, which indicate the different physical origin of these phenomena. For example, the effect in perpendicular magnetic field is seen at lower temperatures ($50\ \mathrm{mK} < T < 2\ \mathrm{K}$). In addition, and maybe more important, we do not observe the enhanced Hall slope in quasiparallel magnetic field for p-type wide PQW. This last observation is crucial for separation of these two effects. For example, naively, we can try to explain the enhanced Hall slope in parallel magnetic fields by redistribution of the charge due to Hartree term for quasi-three-dimensional electrons, as we do in perpendicular magnetic field. However, we would expect in that case that such a three-dimensional electron slab would be wider in the presence of a parallel magnetic field than a 2D slab in zero field because of the Lorentz force, which pushes electrons to the border of the well. Therefore, the density should increase in 3D electron system, which disagrees with our results. In p-type PQW, a spin valve effect is not observed, since the g factor in these system does not change the sign, as in electronic PQW. It agrees with our previous interpretation reported in Ref. 21.

V. CONCLUSION

We describe the measurements of the Hall coefficient in wide n- and p-type PQWs in perpendicular magnetic fields. We observe a strongly enhanced slope of the Hall resistance, especially in hole systems. We attribute this effect to the redistribution of the charge between the well and donor layers, since the exchange-correlation terms and, consequently, potential shape are sensitive to the magnetic field. A variation of the electronic slab width in wide wells has been predicted in several papers.[7,13] However, until now, this effect had not been observed experimentally. Our observation demonstrate the importance of many-body effects in strong magnetic fields, and, in principle, the effect may be considered as a precursor of the CDW instability, which has also been predicted in a wide PQW.

ACKNOWLEDGMENTS

Support of this work by FAPESP and CNPq (Brazilian agencies) is acknowledged.

[1] B. I. Halperin, Jpn. J. Appl. Phys., Suppl. **26**, 1913 (1987).
[2] *The Quantum Hall Effect*, edited by R. E. Prange and S. M. Girvin (Springer-Verlag, New York, 1990).
[3] M. P. Lilly, K. B. Cooper, J. P. Eisenstein, L. N. Pfeiffer, and K. W. West, Phys. Rev. Lett. **82**, 394 (1999); W. Pan, R. R. Du, H. L. Stormer, D. C. Tsui, L. N. Pfeiffer, K. W. Baldwin, and K. W. West, *ibid.* **83**, 820 (1999).
[4] L. Brey, Phys. Rev. B **44**, 3772 (1991).
[5] D.-W. Wang, S. Das Sarma, E. Demler, and B. I. Halperin, Phys. Rev. B **66**, 195334 (2002).
[6] L. Brey and H. A. Fertig, Phys. Rev. B **62**, 10268 (2000).
[7] C. E. Hembree, B. A. Mason, A. Zhang, and J. A. Slinkman, Phys. Rev. B **46**, 7588 (1992).
[8] A. J. Rimberg and R. M. Westervelt, Phys. Rev. B **40**, 3970 (1989).
[9] G. M. Gusev, A. A. Quivy, T. E. Lamas, J. R. Leite, O. Estibals, and J. C. Portal, Phys. Rev. B **67**, 155313 (2003).
[10] T. E. Lamas, A. A. Quivy, C. S. Sergio, G. M. Gusev, and J. C. Portal, J. Appl. Phys. **97**, 076107 (2005).
[11] H. L. Stormer, A. Chang, D. C. Tsui, J. C. M. Hwang, A. C. Gossard, and W. Wiegmann (unpublished).
[12] T. S. Lay, J. J. Heremans, Y. W. Suen, M. B. Santos, K. Hirakawa, M. Shayegan, and A. Zrenner, Appl. Phys. Lett. **62**, 3120 (1993).
[13] J. Dempsey and B. I. Halperin, Phys. Rev. B **47**, 4662 (1993).
[14] E. F. Schubert, J. M. Kuo, R. F. Kopf, A. S. Jordan, H. S. Luftman, and L. C. Hopkins, Phys. Rev. B **42**, 1364 (1990).
[15] V. M. S. Gomes, A. S. Chaves, J. R. Leite, and J. M. Worlock, Phys. Rev. B **35**, 3984 (1987).
[16] M. P. Stopa and S. Das Sarma, Phys. Rev. B **47**, 2122 (1993).
[17] G. Edwards, E. C. Valadares, and F. W. Sheard, Phys. Rev. B **50**, 8493 (1994).
[18] G. Goldoni and F. M. Peeters, Phys. Rev. B **51**, 17806 (1995).
[19] E. Zaremba, Phys. Rev. B **45**, 14143 (1992).
[20] G. Zala, B. N. Narozhny, and I. L. Aleiner, Phys. Rev. B **64**, 201201(R) (2001).
[21] G. M. Gusev, C. A. Duarte, A. A. Quivy, T. E. Lamas, J. R. Leite, A. K. Bakarov, and A. I. Toropov, Phys. Rev. B **71**, 165311 (2005).